

36B, 68 (1971).

<sup>6</sup>C. D. Bowman, G. F. Auchampaugh, and S. C. Fultz, Phys. Rev. **133**, B676 (1964).

<sup>7</sup>See the review of E. Hayward, *Photonuclear Reactions*, National Bureau of Standards Monograph No. 118 (U.S. GPO, Washington, D.C., 1970), p. 6.

<sup>8</sup>H. E. Jackson and K. J. Wetzell, Phys. Rev. Lett. **22**, 1008 (1969).

<sup>9</sup>M. Danos, Nucl. Phys. **5**, 23 (1958).

<sup>10</sup>H. Arenhövel and E. Hayward, Phys. Rev. **165**, 1170 (1968).

<sup>11</sup>H. Arenhövel, private communication.

<sup>12</sup>E. Ambler, E. G. Fuller, and H. Marshak, Phys. Rev. **138B**, 117 (1965).

<sup>13</sup>M. A. Kelly, B. L. Berman, R. L. Bramblett, and S. C. Fultz, Phys. Rev. **179**, 1194 (1969).

## Coincidence Electroproduction in the Region of the $\rho$ Meson\*

E. D. Bloom, R. L. A. Cottrell, H. DeStaebler, C. L. Jordan, G. Miller,† H. Piel,‡  
C. Prescott, R. Siemann, C. K. Sinclair, S. Stein, and R. E. Taylor  
Stanford Linear Accelerator Center, Stanford University, Stanford, California 94305  
(Received 8 December 1971)

Cross sections for the reaction  $ep \rightarrow epX^0$ , measured by detecting both the scattered electron and the proton, are given for missing masses  $m_x$  between 0 and 1 GeV/c<sup>2</sup>. Enhancements are observed at  $m_x=0$  and in the region of the  $\rho$  meson at  $q^2=0.1$  and 0.5 (GeV/c)<sup>2</sup>. The electroproduction of all states with  $m_x$  between 0.7 and 0.83 GeV/c<sup>2</sup> varies like  $e^{-\gamma_5 t}$  for  $q^2=0.1$  (GeV/c)<sup>2</sup>, similar to missing-mass photoproduction, but for  $q^2=0.5$  (GeV/c)<sup>2</sup> it varies like  $e^{-3.5t}$ . In this mass region the resolution tail of the large bremsstrahlung peak at  $m_x=0$  is small.

This Letter reports the results of an inelastic electron scattering experiment at Stanford Linear Accelerator Center (SLAC) where a final-state proton was detected in coincidence with the scattered electron,  $ep \rightarrow epX$ . The experiment attempts to study the electroproduction of the  $\rho$  meson to compare it with photoproduction and to look for new characteristics as the photon becomes more virtual which might give insight into the results of single-arm inelastic electron-proton scattering.

The measured variables are  $E_0$ , the incident electron energy;  $E'$ ,  $\theta$ , and  $\varphi$ , the momentum, polar scattering angle, and azimuthal angle of the scattered electron; and  $P_p$ ,  $\theta_p$ , and  $\varphi_p$ , the corresponding proton variables. These measurements uniquely determine  $m_x$ , the mass of the unobserved state  $X$ :

$$m_x^2 = 2|\vec{q}| |\vec{P}_p| \cos\theta_{\gamma p} - q^2 - t(1 + \nu/M_p),$$

where  $q^2 = 4E_0E' \sin^2(\theta/2)$  is minus the square of the four-momentum transfer from the electron,  $\nu = E_0 - E'$ ,  $|\vec{q}| = (q^2 + \nu^2)^{1/2}$ , and  $t = 2M_p T_p$  is minus the square of the four-momentum transfer to the proton.  $T_p$  is the kinetic energy of the proton,  $M_p$  is its mass, and  $\theta_{\gamma p}$  is the angle between  $\vec{P}_p$  and  $\vec{q}$ .

The cross section can be written<sup>1</sup>

$$\frac{d^6\sigma}{d\Omega dE' dt dm_x d\varphi_q} = \Gamma_T \frac{d^3\sigma_{\text{abs}}}{dt dm_x d\varphi_q},$$

where  $\Gamma_T$  is the flux of virtual photons and  $\varphi_q$  is the azimuthal angle of  $\vec{P}_p$  around  $\vec{q}$  with respect to the electron scattering plane.  $d^3\sigma_{\text{abs}}/dt dm_x d\varphi_q$  then represents the absorption of photons of mass  $q^2$  and energy  $\nu$  with a polarization parameter which is near unity for this experiment.

During the experiment,  $E_0$  and  $E'$  were fixed at 20 and 13 GeV, respectively. Two values of  $\theta$  were used, 1.124° and 2.51°, corresponding to  $q^2=0.1$  and 0.5 (GeV/c)<sup>2</sup>. At each angle data were taken for values of  $t$  between 0.15 and 0.75 (GeV/c)<sup>2</sup>, and, for three points with constant  $q^2$  and  $t$ , sweeps in  $m_x$  were made by varying the proton angle. The resolution in  $m_x$  was dominated by multiple scattering in the hydrogen target. This resolution was determined experimentally by measuring elastic  $e-p$  scattering. At a proton momentum of 0.4 GeV/c the resolution was  $\pm 32$  MeV/c<sup>2</sup>. At 0.96 GeV/c the resolution improved to  $\pm 25$  MeV/c<sup>2</sup>.

The target was a 2-in.-diam cylindrical shell 10 in. long, filled with liquid hydrogen, with its axis parallel to the beam line. To reduce multiple scattering of the protons, the target was moved so that the scattered protons traversed as little liquid hydrogen as possible (approximately 1 cm). The length of the target seen by the 1.6-GeV spectrometer depended on the opening of tungsten slits at the entrance of the spectrometer. These slits were always adjusted to exclude

events from the end walls of the target. Experimentally, the coincidence yield from an identical target cell containing no hydrogen was always less than 1% of the full target yield.

Protons were cleanly identified in the 1.6-GeV spectrometer<sup>2</sup> by size of the pulse height from a 1-in.-thick scintillation counter, time of flight, and the lack of a signal in a 2-in.-thick Lucite Cherenkov counter. Three scintillation-counter hodoscopes gave resolutions of  $\pm 0.25\%$  in momentum,  $\pm 1.1$  mrad in the horizontal projected angle, and  $\pm 7.5$  mrad in the vertical projected angle.

The positions and angles of the scattered electron after passing through the 20-GeV spectrometer<sup>3</sup> were measured in five proportional wire chambers.<sup>4</sup> The resolutions were  $\pm 0.05\%$  in momentum and  $\pm 0.05$  mrad in both projected angles. Electrons were cleanly identified with a lead-Lucite shower counter.

The coincidence timing was done between single scintillation counters, each counter having a photomultiplier tube on both ends. The difference in time of the signals from each set of photomultiplier tubes was measured by time-to-amplitude converters and stored on tape with other event information. The distribution of true coincidence events was approximately 10 nsec wide. The other event information permitted corrections to be made to these time differences for the following effects: (a) path-length differences for differing kinematics, (b) velocity differences, (c) finite size of the timing counters, (d) pulse-height variations, and (e) ionization losses after momentum analysis. The two semi-independent measurements were then averaged to form the final time spectrum. The final timing resolution was momentum dependent because of multiple scattering and the resolution of the proton hodoscope. At a proton momentum of 0.4 GeV/c the timing resolution obtained was 1.6 nsec full width at half-maximum and at 0.96 GeV/c it was 0.8 nsec.

To determine the proper time cut for each momentum, electron bunches were accelerated, separated by 12.5, 25, or 50 nsec. The length of a bunch was 5 psec so that both true and accidental coincidences provided information about the timing resolution. This allowed optimization of the corrections to the timing signals in regions with a low rate of true coincidences. Further, the time-to-amplitude converters were calibrated using the accurately known bunch spacing.

The electron fluxes of  $10^7$ - $10^9$  per 1.6- $\mu$ sec pulse were measured by a secondary-emission

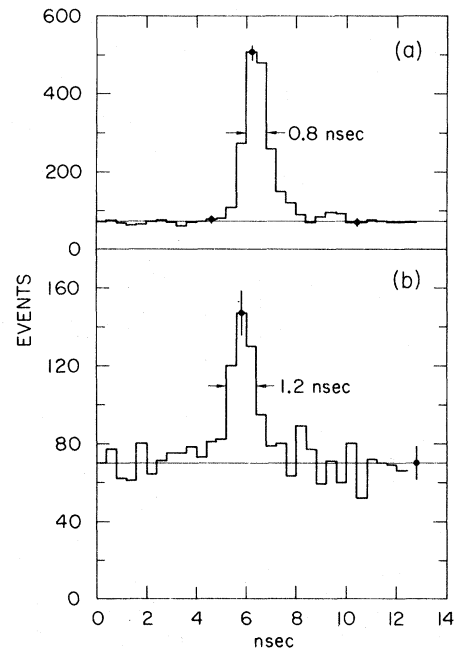


FIG. 1. The timing spectrum for (a)  $m_x=0$ ,  $q^2=0.5$  (GeV/c)<sup>2</sup>, and  $t=0.76$  (GeV/c)<sup>2</sup>, and (b)  $m_x=m_\rho$ ,  $q^2=0.5$  (GeV/c)<sup>2</sup>, and  $t=0.5$  (GeV/c)<sup>2</sup>.

quantameter. At these fluxes, the ratio of the total number of true coincidence events to the random events within the time cuts was more than 100:1 for elastic  $e-p$  scattering, approximately 5:1 for bremsstrahlung [see Fig. 1(a)], and between 1:1 and 0.3:1 for the  $\rho$  mass region [see Fig. 1(b)].

The systematic uncertainty of the subtraction of random events from the yield was estimated to be less than 10% by studying the variation of the yield with the size of the time cut. This estimate includes a study of effects due to beam structure with time.

The sixfold double-arm acceptance  $\int d\Omega dE' dm_x \times dq_q$  was calculated by a Monte Carlo program from models of the two spectrometers based on beam-optics measurements. Single-arm elastic-scattering measurements with the 20-GeV spectrometer agreed with world-average form factors to an accuracy of  $\pm 5\%$ . Single-arm 1.6-GeV measurements of elastic  $e-p$  scattering agreed to within the systematic uncertainty of  $\pm 10\%$ . The systematic error in the coincidence cross-section normalization is estimated to be less than  $\pm 20\%$ .

Figure 2 shows the three measured spectra of sixfold differential cross sections as a function of missing mass. Since the cross section at  $m_x=0$  is approximately fifty times larger than the rest of the spectrum, only the data for  $m_x > 0.1$

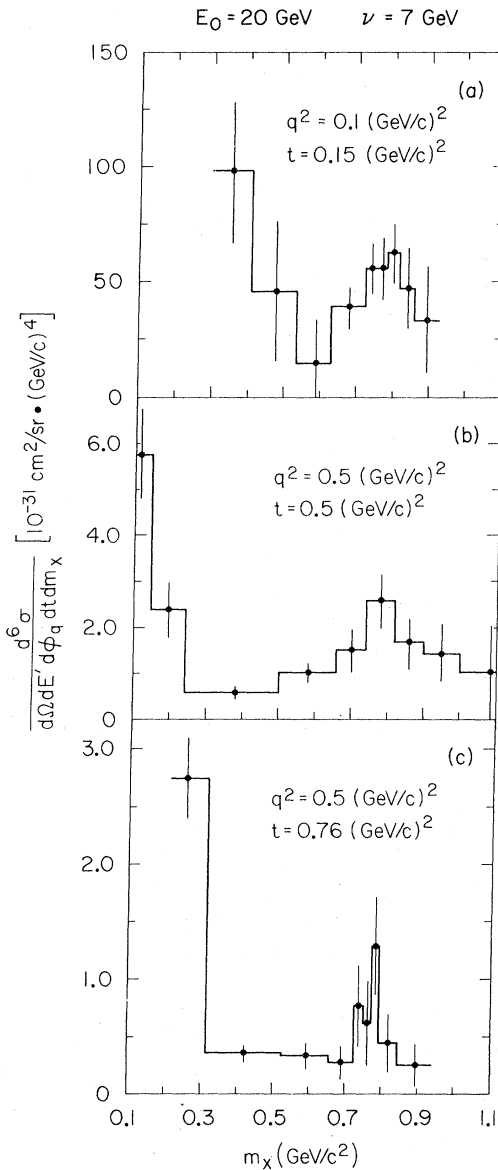


FIG. 2. The sixfold differential cross section as a function of missing mass for three values of  $q^2$ ,  $\nu$ , and  $t$ .

$\text{GeV}/c^2$  are shown. Besides the large peak at  $m_x = 0$ , which, within the 20% normalization uncertainty, can be attributed to the process  $ep \rightarrow ep\gamma$ , all three spectra show enhancements in the neighborhood of the  $\rho$ -meson mass. Broadening of the  $m_x \approx 0$  peak due to the emission of multiple soft photons is small compared to the broadening due to experimental resolution. At the  $\rho$  mass, the contribution from the  $m_x \approx 0$  peak is estimated to be  $\leq 20\%$ .

Additional measurements were made concentra-

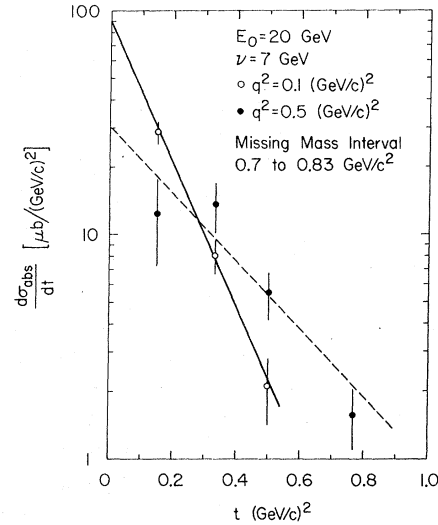


FIG. 3. The cross section  $d\sigma_{\text{abs}}/dt = 2\pi \int (d^3\sigma_{\text{abs}}/dt d\varphi_a \times dm_x) dm_x$ . The solid line is the fit to the  $q^2 = 0.1$ - $(\text{GeV}/c)^2$  data given by  $(91.1 \pm 18) \exp[-(7.5 \pm 0.8)t] \mu\text{b}/(\text{GeV}/c)^2$ . The dashed line is the fit to the  $q^2 = 0.5$ - $(\text{GeV}/c)^2$  data given by  $(30.5 \pm 9.4) \exp[-(3.5 \pm 0.6)t] \mu\text{b}/(\text{GeV}/c)^2$ .

ting on the mass region between 0.7 and 0.83  $\text{GeV}/c^2$ . This region is centered on the mass of the  $\rho$  meson, but it included the  $\omega$  meson, any nonresonant background, and the resolution tail from the  $m_x = 0$  region. For  $q^2 = 0.1$   $(\text{GeV}/c)^2$ , data were taken at  $t = 0.33$  and  $0.5$   $(\text{GeV}/c)^2$ , and for  $q^2 = 0.5$   $(\text{GeV}/c)^2$ , at  $t = 0.15$  and  $0.33$   $(\text{GeV}/c)^2$ .

The acceptance in  $\varphi_a$  was momentum dependent and ranged between 0.6 and 1.2 rad, centered about 0. The angular distributions appear to be flat, but the data do not rule out a dependence like  $\cos 2\varphi_a$ .

For  $q^2 = 0.1$   $(\text{GeV}/c)^2$ , the cross-section dependence on  $t$  seen in Fig. 3 is similar to that found in missing-mass photoproduction in this region<sup>5</sup> and is well fitted by the form  $e^{-bt}$ , where  $b = 7.5 \pm 0.8$   $(\text{GeV}/c)^{-2}$ . However, the variation at  $q^2 = 0.5$   $(\text{GeV}/c)^2$  is markedly different from photoproduction. If the points are fitted by an exponential form  $e^{-bt}$ , then  $b = 3.5 \pm 0.6$   $(\text{GeV}/c)^{-2}$ . The probability of observing a  $\chi^2$  larger than obtained is 60% for  $q^2 = 0.1$   $(\text{GeV}/c)^2$  and 13% for  $q^2 = 0.5$   $(\text{GeV}/c)^2$ . The observed flattening of the  $t$  dependence with increasing  $q^2$  has been speculated upon by various authors.<sup>6</sup>

Assuming that an exponential form accurately describes the  $t$  dependence, and that the distribution in  $\varphi_a$  is flat, as would be expected for a diffractive production mechanism,<sup>1</sup> the ratio of the integrated contribution of the mass region from

0.7 to 0.83 GeV/c<sup>2</sup> to single-arm deep inelastic scattering<sup>7</sup> at  $q^2 = 0.1$  (GeV/c)<sup>2</sup> is  $(10.7 \pm 1.3)\%$  which is consistent with photoproduction. At  $q^2 = 0.5$  (GeV/c)<sup>2</sup> this ratio is  $(16.5 \pm 3.0)\%$ . The assumption of exponential behavior is important since at both  $q^2$  values more than 50% of the integral comes from  $t$  values lower than those measured.

The statistics are marginal for answering the interesting question of how much  $\rho$  signal is present in the mass region from 0.7 to 0.83 GeV/c<sup>2</sup>. Fits were made to the mass spectra in Figs. 2(a), 2(b), and 2(c) using a single Breit-Wigner resonance shape plus a naive background of the form  $(m_x - m_{2\pi})(m_{\max} - m_x)$ , where  $m_{\max}$  is the highest missing mass allowed by kinematics. The mass and width of the Breit-Wigner were fixed at 765 and 140 MeV, respectively. At  $q^2 = 0.1$ ,  $t = 0.15$  (GeV/c)<sup>2</sup>, and  $m_x = m_\rho$ , we find the resonant fraction of the cross section to be  $(55 \pm 30)\%$ . At  $q^2 = 0.5$  (GeV/c)<sup>2</sup> we obtain  $(47 \pm 30)\%$  for  $t = 0.5$  (GeV/c)<sup>2</sup> and  $(75 \pm 40)\%$  for  $t = 0.76$  (GeV/c)<sup>2</sup>.

We have made no radiative corrections to the data presented here. In a model calculation, events with a  $\rho$ -mass distribution were simulated by a Monte Carlo program and the effects of soft-photon emission were taken into account. The mass region between 0.7 and 0.83 GeV/c<sup>2</sup> was depleted by 35–50%. This depletion was  $t$  and  $q^2$  dependent, and its size further complicates the interpretation of the integrated cross sections given above. However, the slopes of the experimental  $t$  dependence were not affected outside of the errors given.

This experiment is similar to a previously published experiment at Cornell<sup>8</sup> where data were taken under different kinematical conditions. Further experiments are necessary to resolve questions like photon shrinkage.<sup>6</sup>

We would especially like to thank the Spectrometer Facilities Group at SLAC for their constant support, Group F at SLAC for sharing their knowledge of the 1.6-GeV spectrometer, Mac D. Mestayer for his assistance during the data taking, G. Johnson, K. Doty, W. Weeks, R. Haley, and S. Sund for their expert technical help, and the accelerator crew for one of the steadiest beams on record.

\*Work supported by the U. S. Atomic Energy Commission.

†Present address: University of Washington, Seattle, Wash. 98105.

‡Present address: Bonn University, Bonn, Germany.  
<sup>1</sup>H. Fraas and D. Schildknecht, Nucl. Phys. **B14**, 543 (1970).

<sup>2</sup>R. Anderson *et al.*, Nucl. Instrum. Methods **66**, 328 (1968).

<sup>3</sup>W. K. H. Panofsky, in *Proceedings of the International Symposium on Electron and Photon Interactions at High Energies, Hamburg, Germany, 1965* (Springer, Berlin, 1965).

<sup>4</sup>E. Bloom, R. L. A. Cottrell, G. Johnson, C. Prescott, R. Siemann, and S. Stein, SLAC Report No. SLAC-PUB-981 (unpublished).

<sup>5</sup>D. L. Kreinick, Ph.D. dissertation, California Institute of Technology, 1970 (unpublished).

<sup>6</sup>H. Cheng and T. T. Wu, Phys. Rev. **183**, 1324 (1969); R. W. Griffith, Phys. Rev. **188**, 2112 (1969); J. D. Bjorken, SLAC Report No. SLAC-PUB-905 (unpublished).

<sup>7</sup>E. D. Bloom *et al.*, SLAC Report No. SLAC-PUB-653 (unpublished); and preliminary results at 4° from SLAC, Group A, reported to the Fifth International Conference on Electron and Photon Interactions at High Energies, Cornell, 1971 (unpublished). The values of  $d^2\sigma/d\Omega dE'$  at  $E_0 = 20$  GeV,  $\nu = 7$  GeV, and  $q^2 = 0.1$  (GeV/c)<sup>2</sup> and 0.5 (GeV/c)<sup>2</sup> used are  $2.0 \times 10^{-29}$  cm<sup>2</sup>/sr GeV and  $1.9 \times 10^{-30}$  cm<sup>2</sup>/sr GeV, respectively.

<sup>8</sup>D. E. Andrews *et al.*, Phys. Rev. Lett. **26**, 864 (1971), and Laboratory for Nuclear Studies, Cornell University, Report No. CLNS-169 (unpublished).